UDC 621.3 https://doi.org/10.20998/2074-272X.2025.3.04

H. Chaib, S. Hassaine, Y. Mihoub, S. Moreau

Intelligent power control strategy based on self-tuning fuzzy MPPT for grid-connected hybrid system

Introduction. *This paper investigates various methods for controlling the Maximum Power Point Tracking (MPPT) algorithm within the framework of intelligent energy control for grid-connected Hybrid Renewable Energy Systems (HRESs).* ***The purpose*** *of the study is to improve the efficiency and reliability of the power supply in the face of unpredictable weather conditions and diverse energy sources. Intelligent control techniques are used to optimize the extraction of energy from available sources and effectively regulate energy distribution throughout the system.* ***Novelty*** *study is employing intelligent control strategies for both energy optimization and control. This research distinguishes itself from conventional approaches, particularly through the application of Self-Tuning Fuzzy Logic Control (ST-FLC) and fuzzy tracking. Unlike conventional methods that rely on logical switches, this intelligent strategy utilizes fuzzy rules adapted to different operating modes for more sophisticated energy control. The proposed control strategy minimizes static errors and ripples in the direct current bus and challenges in meeting load demands.* ***Methods*** *of this research includes a comprehensive analysis of several optimization techniques under varying weather scenarios. The proposed strategy generates three control signals that correspond to selected energy sources based on solar irradiation, wind velocity and battery charging status.* ***Practical value.*** *ST-FLC technique outperforms both conventional methods and standard Fuzzy Logic Controllers (FLCs). It consistently delivers superior performance during set point and load disturbance phases. The simulation, conducted using MATLAB/Simulink.* ***The results*** *indicate that fuzzy proposed solution enables the system to adapt effectively to various operational scenarios, displaying the practical applicability of the proposed strategies. This study presents a thorough evaluation of intelligent control methods for MPPT in HRESs, emphasizing their potential to optimize energy supply under varying conditions.* References 27, tables 6, figures 18.

Key words: **maximum power point tracking algorithm, hybrid renewable energy system, conventional controller, fuzzy logic controller, self-tuning fuzzy logic control.**

Вступ. *У цій статті досліджуються різні методи керування алгоритмом стеження за точкою максимальної потужності (MPPT) в рамках інтелектуального керування енергією для підключених до мережі гібридних систем відновлюваної енергетики (HRESs).* ***Метою*** *дослідження є підвищення ефективності та надійності електропостачання в умовах непередбачуваних погодних умов та різноманітних джерел енергії. Інтелектуальні методи управління використовуються для оптимізації видобутку енергії з доступних джерел та ефективного регулювання розподілу енергії по всій системі.* ***Новизна*** *дослідження полягає у застосуванні інтелектуальних стратегій управління як для оптимізації, так і для контролю енергії. Це дослідження відрізняється від традиційних підходів, зокрема, завдяки застосуванню самонастроюваного нечіткого логічного керування (ST-FLC) та нечіткого відстеження. На відміну від традиційних методів, які покладаються на логічні перемикачі, це інтелектуальне управління використовує нечіткі правила, адаптовані до різних режимів роботи для більш складного управління енергією. Запропонована стратегія керування мінімізує статичні похибки та пульсації в шині постійного струму, а також проблеми з задоволенням потреб навантаження.* ***Методи*** *дослідження включають комплексний аналіз декількох методів оптимізації за різних погодних умов. Запропонована стратегія генерує три сигнали керування, які відповідають обраним джерелам енергії на основі сонячного випромінювання, швидкості вітру та стану заряду акумуляторів.* ***Практична цінність****. Технологія ST-FLC перевершує як традиційні методи, так і стандартні контролери нечіткої логіки (FLC). Вона стабільно забезпечує високу продуктивність під час фаз заданого значення та збурення навантаження. Моделювання проводилося за допомогою MATLAB/Simulink.* ***Результати*** *показують, що запропоноване нечітке рішення дозволяє системі ефективно адаптуватися до різних сценаріїв роботи, демонструючи практичну застосовність запропонованих стратегій. Це дослідження представляє ретельну оцінку інтелектуальних методів управління для MPPT в HRES, підкреслюючи їх потенціал для оптимізації енергопостачання за різних умов.* Бібл. 27, табл. 6, рис. 18.

Ключові слова: **алгоритм стеження за точкою максимальної потужності, гібридна система відновлюваної енергетики, традиційний регулятор, регулятор нечіткої логіки, самонастроюваний регулятор нечіткої логіки.**

Introduction. In light of the massive increase in population, the demand for energy has increased, obliging people to think about new non-traditional energy sources. Conventional energy sources are exhaustible and not ecology friendly due to the carbon dioxide CO_2 emissions, in addition to this their market is not stable. The trend is towards renewable energies in particular solar, wind and hydrogen. Renewable energy has various advantages such as being free, sustainable and respecting environment. In the other side, there is non-linearity and intermittence caused by climatic conditions. To overcome this constraint, great achievement in power sector has been deployed. Wind and solar are the most exploited renewable resources [1]. The stability of the grid depends on the equilibrium between consumption and production. The widespread use of renewable energies must be supported by the use of additional electrical energy storage devices. The Hybrid Renewable Energy Systems (HRESs) that runs mostly on solar and wind energy is commonly used. There are two configurations standalone or grid connected [2–4].

A number of works has been reported to study power control. Electrification and microgrids are treated in [5, 6], smart grids – in [7]. Various configurations of HRESs often consist of energy sources (wind energy and solar energy), in addition to storage systems with the possibility of connecting to the grid or standalone. Fuzzy Logic Control (FLC), Perturb and Observe (P&O), hill climbing and incremental conductance have been most used for photovoltaic (PV) Maximum Power Point Tracking (MPPT) [8–11]. To extract the maximum energy from Wind Turbines (WTs) the most used configuration are realized by rectifier or by chopper. Several studies have been developed using classic control method (PI, PID, sliding mode control so on) or artificial intelligence (FLC, Self-Tuning Fuzzy Logic Control (ST-FLC), neural network and genetic algorithms) [12–16].

In general, the energy control is still based on checks and balances. A number of studies have proposed different methods of power control [17–24].

Literature review. The paper [25] discusses the use of a ST-FLC PID controller for MPPT in variable-speed

WTs. While the proposed controller enhances MPPT performance, it still exhibits static errors and ripples at the DC bus. In [26], energy control strategies for HRESs with battery storage are examined. This hybrid system, comprising PV panels, WTs and diesel generators, operates without grid connection. A FLC is implemented to optimize power allocation among the PV, WT, diesel and battery systems. However, the established rules fail to effectively manage power distribution among sources and battery storage, leading to challenges in meeting load demands. The study [27] presents a PI controller for energy control in HRES. Despite its application, this conventional regulator struggles with disturbances in the DC voltage. Additionally, the mathematical models based on PI control calculate the gains for a nonlinear system. This approach suffers from static errors at the DC bus level and experiences significant voltage spikes during system startup.

The goal of the article is to improve the energy efficiency and reliability of the power supply in various and unpredictable weather conditions. Intelligent (FLC and ST-FLC) MPPT strategies are suggested and compared to conventional (PI and P&O) MPPT. An intelligent power control system based on fuzzy rules adapted to different operating modes of a HRESs with battery storage. The control also minimizes static errors and ripples in the direct current bus.

The suggested algorithms are employed to regulate the output voltage to a predefined value in order to extract the maximum possible power from WT and PV systems. A FLC is used to act on the HRES according to the proposed intelligent strategy. The FLC has many advantages over conventional strategies based mainly on logical states. It is simple and very close to human reasoning. The main advantage is that expert knowledge is captured and used at any time to improve the existing system by adding some rules or acting on the power organization controller for accurate selection of the source at the right time to feed the telecommunication loads and manage the whole hybrid power system. The different control strategies developed were implemented in the MATLAB/Simulink environment. The obtained results showed that the ST-FLC technique is superior to the others, and the results confirm the superiority of FLC to supervise the system according to the proposed strategy.

System description. The studied HRES is connected to the grid and has two renewable energy sources (PV and WT) with storage. The power tracking is based on FLC. The purpose is to match the power demand of the load and to keep the battery bank in a state of charge in order to prevent power outages and to extend the lifetime of the batteries independently of fluctuations in solar irradiation and wind velocity. The design of the presented system is shown in Fig. 1.

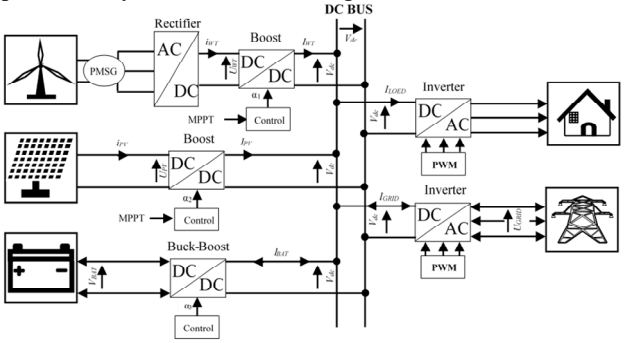

Fig. 1. Hybrid power system

WT system model. The WT-derived mechanical energy is detailed as follows:

$$P_m = \tfrac{1}{2}\rho\pi R^2 V_w^3 c_p(\lambda,\beta), \quad (1)$$

where P_m is the power extracted from the WT; ρ is the density of the air; R is the radius of the blade; V_w is the wind velocity; $C_p(\lambda, \beta)$ is the power coefficient, where λ is the tip speed ratio. The definition of the parameter λ is:

$$\lambda = \omega_m R / V_w . \quad (2)$$

The pitch angle β is maintained constant during MPPT control ($\beta = 0$), ω_m is the mechanical speed of the WT. The input torque for the turbine is:

$$T_m = P_m / \omega_m . \quad (3)$$

The generator is modelled by the following voltage equations in d_q-axis:

$$V_{sd} = R_s I_{sd} + \frac{\mathrm{d}\phi_{sd}}{\mathrm{d}t} + \omega_e \phi_{sq}; \quad (4)$$

$$V_{sq} = R_s I_{sq} + \frac{\mathrm{d}\phi_{sq}}{\mathrm{d}t} + \omega_e \phi_{sd}, \quad (5)$$

where i_{sd}, i_{sq} are the currents in the d-q reference frame; R_s is the stator resistance; ω_e is the electrical rotation speed; φ_{sd} along with φ_{sq} indicate the stator flux linkages along the d and q-axis are acquired through:

$$\phi_{sd} = L_d i_{sd} + \varphi_m; \quad (6)$$

$$\phi_{sq} = -L_q i_{sq}, \quad (7)$$

where L_d, L_q are the inductances in the d-q reference frame; ϕ_m is the rotor magnetic flux generated by the generator.

The electromagnetic torque expression T_e is:

$$T_e = \tfrac{3}{2} p(L_d - L_q) i_{sd} i_{sq} + \phi_m i_{sq}, \quad (8)$$

where p is the number of pole pairs.

The mechanical equation connecting the generator and WT is:

$$J_{eq} \frac{\mathrm{d}w_g}{\mathrm{d}t} = T_e + T_l - B_m w_g, \quad (9)$$

where J_{eq} is the equivalent inertia moment of the system; w_g is the angular speed of the generator; T_e is the electromagnetic torque produced by the generator; T_l is the torque exerted by the turbine on the generator; B_m is the viscous damping coefficient.

PV system model. Figure 2 shows the equivalent circuit of a standalone solar cell, which includes a single diode, and, using Kirchhoff's current law, the output current I_{pv} of the solar PV cell can be expressed as:

$$I_{pv} = I_{ph} - I_d - I_{sh}; \quad (10)$$

$$I_d = I_0\left(\exp\left[\frac{V_{pv}}{nV_t}\right] - 1\right); \quad V_t = \frac{kT}{q}, \quad (11)$$

$$I_{pv} = I_{ph} - I_0\left(\exp\left[\frac{q(V_{pv} + R_s I_{pv})}{nkT}\right] - 1\right) - \frac{V_{pv} + R_s I_{pv}}{R_{sh}}, \quad (12)$$

where I_d is the current through the diode; I_{sh} is the current through the resistor R_{sh}; R_s, R_{sh} are the series and shunt resistances, respectively; I_0 is the saturation current; I_{ph} is the photocurrent; n is the diode ideality factor; V_t is the thermal voltage of the diode; k is the Boltzmann constant; T is the operating temperature of the cell; q is the electron charge.

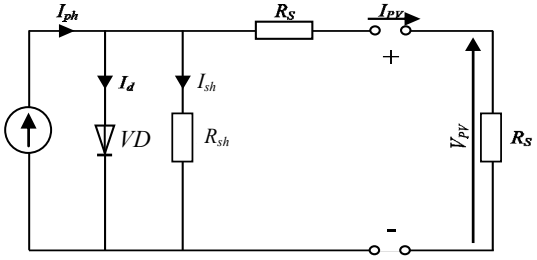

Fig. 2. Equivalent circuit of solar cell

Storage modelling. It is based on the electrical diagram (Fig. 3), containing 3 elements: a voltage source, the internal resistance and the capacitor:

$$U_{bat} = E_0 - K.\frac{\int I_b dt}{Q_0} + R_b I_b , \qquad (13)$$

where E_0 is the open circuit voltage of the battery; K is the battery-dependent constant; R_b is the internal battery resistance; I_b is the discharging current; Q_0 is the battery capacity; $\frac{K}{Q_0}\int I_b \mathrm{d}t$ indicates the battery discharge status.

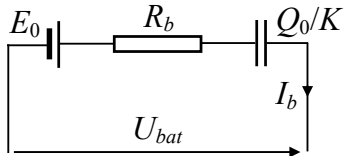

Fig. 3. Electrical model of the battery

Grid model. The dynamic grid connection model, employing a reference frame that synchronously rotates with the grid voltage space vector, is depicted as:

$$U_{gd} = -R_g i_{gd} - \frac{L_g \mathrm{d}i_{gd}}{\mathrm{d}t} - w_{gr} L_g i_{gq} + e_{gd} ; \qquad (14)$$

$$U_{gq} = -R_g i_{gq} - \frac{L_g \mathrm{d}i_{gq}}{\mathrm{d}t} - w_{gr} L_g i_{gd} , \qquad (15)$$

where R_g is the resistance and L_g is the inductance of the filter, with the latter positioned between the converter and the grid; u_{gd}, u_{gq} are the inverter voltage components, while w_{gr} stands for the electrical angular velocity of the grid.

FLC design. The FLC code comprises 3 sections: pre-processing, the fuzzy and interface rule engine, and post-processing. In the pre-processing phase, the fuzzy control (FC) input variables are the rate error (e) and the change in error (Δe). The gain factors for input scale and error scale are denoted as Ge and $G\Delta e$, respectively. The final phase of the FLC system involves post-processing, where the output signal ΔI is scaled by the factors d$u(t)$

$$e(t) = S^*(t) - S(t) ; \qquad (16)$$

$$\Delta e(t) = \frac{e(t) - e(t-1)}{t_{samp}} ; \qquad (17)$$

$$I^* = I^*(t-1) + \mathrm{d}u(t) , \qquad (18)$$

with Mamdani's method, the input fuzzy variables are converted into suitable linguistic values, then treated in the region of the fuzzy set that includes the membership function (MF) where a suitable fuzzy output is obtained using fuzzy rules, and then the fuzzy output is transformed into a crisp value in the defuzzification using the method of centroid, also known as the method of center of gravity given by:

$$\Delta U = \sum_{i=1}^{n} c_i + u_i \Big/ \sum_{i=1}^{n} u_i , \qquad (19)$$

where c_i is the discrete element within an output fuzzy set; u_i is its membership function; n is the total number of fuzzy rules. Upon converting the inputs into linguistic variables, the FLC facilitates a controlled adjustment in the voltage reference, aiming to achieve maximum power, relying on the rules outlined in Table 1.

Table 1

Set of fuzzy rules

dU		ΔE				
		NB	NS	Z	PS	PB
E	NB	NB	NB	NS	NS	Z
	NS	NB	NS	NS	Z	PS
	Z	NS	NS	Z	PS	PS
	PS	NS	Z	PS	PS	PB
	PB	Z	PS	PS	PB	PB

Figure 4 represents the input and output variables' MFs encompass triangular and trapezoidal shapes denoted as Negative Big (*NB*), Negative Small (*NS*), Zero (*Z*), Positive Small (*PS*) and Positive Big (*PB*).

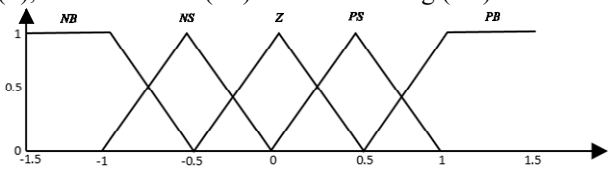

Fig. 4. MFs of e, Δe and Δu

The proposed ST-FLC. Figure 5 shows the overall structure of ST-FLC. The proposed ST-FLC uses a straightforward algorithm that reduces the system complexity and computational burden. The MFs for the 2 normalized inputs (e and Δe) and the output (Δu) of the controller were given on the normalized common area [–1.5, 1.5]. The following are the relationships between the scaling factors (G_e, $G_{\Delta e}$ and G_u) and the ST-FLC input and output variables:

$$e = G_e \times e ; \qquad (20)$$

$$\Delta e = G_{\Delta e} \times \Delta e ; \qquad (21)$$

$$\Delta u = (\beta \times G_u) \times \Delta u , \qquad (22)$$

where:

$$\beta = K_1 (\tfrac{1}{m} + |\Delta e|) . \qquad (23)$$

The variable β is formulated based on the system's expert understanding, following this principle. If the system approaches its desired operating point rapidly (small Δe), the output action (Δu) should be heightened (decreasing G_u) to prevent significant overshoot or undershoot. Conversely, if the system deviates swiftly from the target operating point (large Δe), the output action (Δu) must be increased (augmenting G_u) to restrict these deviations and expedite the system's return to its target operating point. Therefore, β is expressed using this design by adding (Δe) to the fraction ($1/m$) to prevent a lower gain multiplication (G_u) when (Δe) is exceedingly small. A lower gain multiplication could lead to oscillations and non-steady state behavior during steady-state operation. The value of m is set to be equal to the number of fuzzy uniform input partitions (e and Δe) (MF number). The value of K_1 is selected to allow the variation of β, set to 4 during the tuning process. The other fuzzy settings remain unchanged, adhering to the standard fixed parameter FLC.

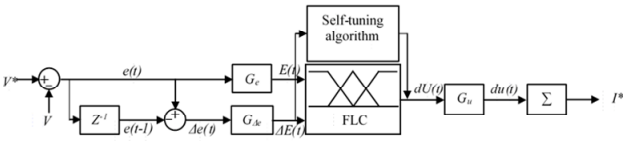

Fig. 5. ST-FLC structure

The proposed MPPT algorithm. Figure 6 represents the proposed MPPT algorithm for WT which based on ST-FLC.

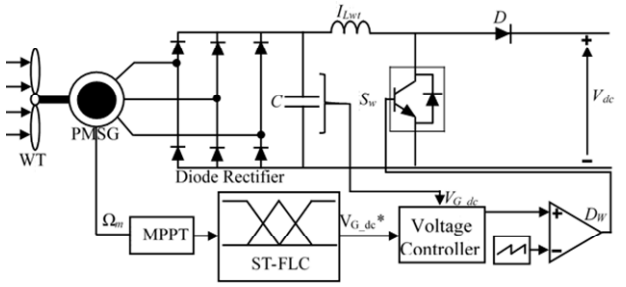

Fig. 6. ST-FLC MPPT of WT control

The MPPT algorithm proposed for solar system is based on ST-FLC is shown in Fig. 7.

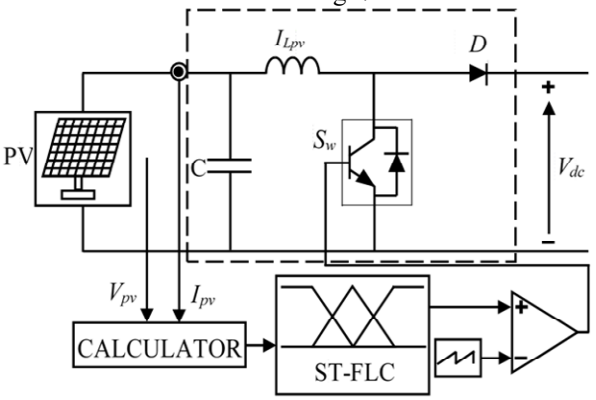

Fig. 7. ST-FLC MPPT of PV control

It relies on the Mamdani input controller. As per the MPPT algorithm, the recommended approach utilizes the error E as input and modifies the output through a distinctive ST algorithm. By taking $E = (D_P/D_V)$ for each step and considering the sign of D_P and D_V, and modify the output, which is the duty cycle dD.

$$if\ E < 0 \text{ then } D = D + \Delta D\ ; \tag{24}$$

$$if\ E > 0 \text{ then } D = D - \Delta D\ ; \tag{25}$$

$$if\ E = 0 \text{ then } D = D\ , \tag{26}$$

where the integrator with forward Euler method (the standard method) to obtain the duty cycle (D); where the gain value k and the sample time T of the integrator were respectively set to 1 and 0.01:

$$D(k) = D(k-1) + kT\mathrm{d}D(k-1)\ . \tag{27}$$

Power control with FC. The hybrid system control strategy must satisfy load demand under various weather conditions and control energy flow while keeping the different energy sources operating efficiently. Figure 8 shows the global system configuration. The FLC inputs are respectively solar irradiation G, wind velocity V_w, battery state of charge (SOC) and load demand. The outputs are switches corresponding to the selected source according to the proposed strategy, which will be explained in power control with FC section.

The scheme parameters are next. **PV generator**: rated power P_{wt} = 2,7 kW. **WT generator**: power rating P_{pv} = 6 kW; power rating of the turbine P_{tur} = 8,5 kW; radius of the turbine R_{tur} = 3.24 m. **Battery bank**: rated voltage V_{bat} = 200 V; capacity C = 100 A·h. **DC bus**: V_{dc} = 630 V. **Load**: minimum power P_l = 1 kW; maximum power P_{lM} = 8 kW. **Grid**: effective voltage value V_g = 220 V; maximum voltage value V_{gM} = 381 V.

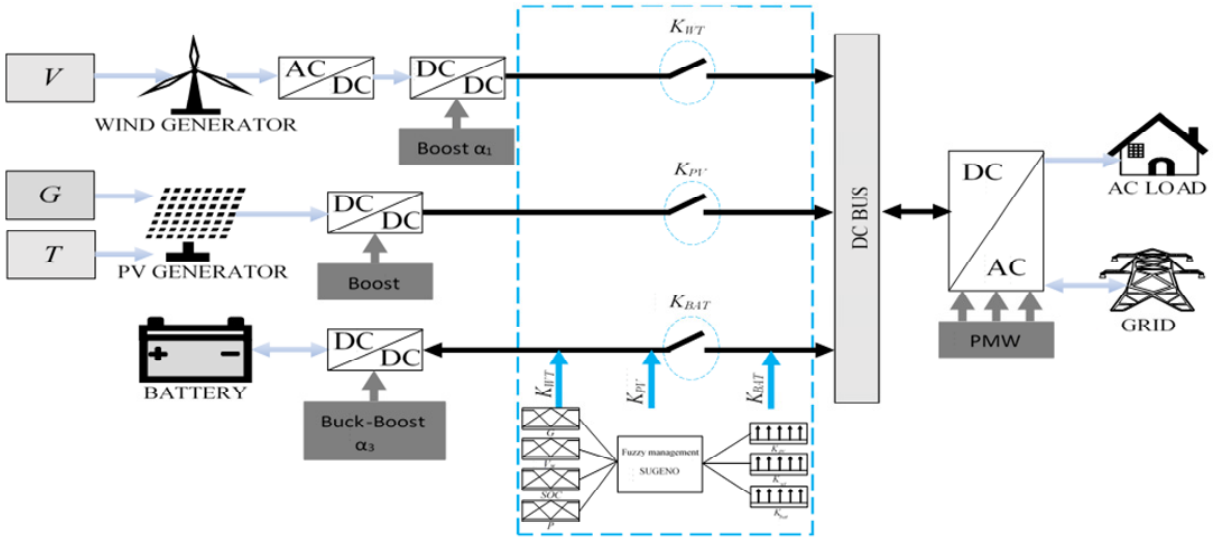

Fig. 8. Power control with FC general structure

The proposed strategy uses the energy produced by PV, WT and battery to satisfy the demands of the load. The FLC principle is to generate 3 signals of control K_{pv}, K_{wt} and K_{bat} from 3 inputs: G, V_w and SOC. K_{pv}, K_{wt} and K_{bat} are the switches that control the PV system, WT and battery, respectively. Table 2 presents the rule table for the fuzzy controller, where the inputs are fuzzy sets representing SOC, V_w and G. The output indicates the states of the 3 switches K_{pv}, K_{wt} and K_{bat}.

Table 2

Interval of fuzzy controller inputs

	Low	Medium	High
SOC, %	0–20	20–95	95–100
V_w, m/s	0–2	2–9	9–12
G, W/m^2	0–200	200–600	600–1000

Depending on the (ON/OFF) states of the K_{pv}, K_{wt} and K_{bat} switches, with the power supplied to the load expressed as:

$$P_{load} + P_{lost} + P_{bat} = P_{wt}K_{wt} + P_{pv}K_{pv}, \qquad (28)$$

where P_{wt}, P_{pv} are the power generated by the WT and the PV system; P_{bat} is the battery power; P_{load} is the power consumed by the load; P_{lost} is the power lost in the system; $P_{bat} > 0$ – when the batteries are charged; $P_{bat} < 0$ – when the batteries are discharged.

To guarantee the effective operation of the system under all conditions, we developed a range of scenarios based on system inputs (V_w, G and SOC) while considering the load. The resulting set is displayed below.

Mode 1 (M1). WT and PV power supply the load, the total energy is enough to power the load and the excess used to charge the batteries. The battery is charging.

Mode 2 (M2). WT and PV energy insufficient to supply the load, in this case, power is supplied by the battery to satisfy the demand. The battery is discharging.

Mode 3 (M3). PV power is the only source, sufficient to satisfy the load and the excess used to charge the batteries, this mode occurs during a sunny day (summer). The battery is charging.

Mode 4 (M4). PV source is insufficient to supply the load. Power is supplied by the battery to satisfy the load demand, the battery is discharging.

Mode 5 (M5). WT energy is the only source, sufficient to satisfy the load and the excess used to charge the batteries, which is the situation on a winter day with no solar radiation or at night with a good wind velocity. The battery is charging.

Mode 6 (M6). WT power source is insufficient to supply the load. Power is supplied by the battery to satisfy the load. The battery is discharging.

Mode 7 (M7). Only the battery powered the load. The battery is discharging.

Mode 8 (M8). No source available and the battery is empty, so the grid therefore supplied the power needed to satisfy the load demand.

Figure 9 shows the flowchart governing the energy control system utilizing the fuzzy system. This fuzzy system processes the inputs shown in Table 2, along with the total energy sum represented in (28). The control system evaluates 4 inputs to determine which mode, as previously described, should be implemented.

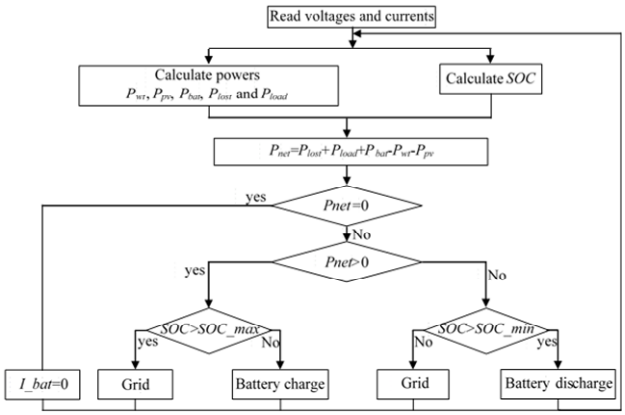

Fig. 9. Flowchart of the power control algorithm

Results simulation analysis. The simulation, conducted in MATLAB/Simulink, assesses the energetic efficiency and feasibility of the proposed strategy across various potential climatic conditions, as depicted in Fig. 8. The selected profiles include wind velocity (Fig. 10) and solar irradiance (Fig. 11).

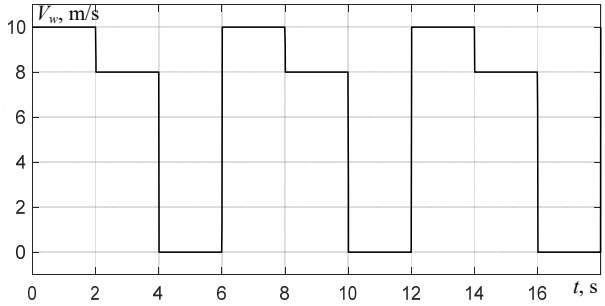

Fig. 10. Profile of the wind velocity

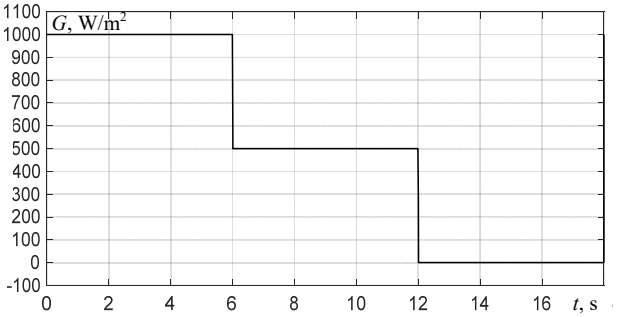

Fig. 11. Profile of the solar irradiation

The speed control response of the ST-FLC exhibits superior tracking characteristics compared to other controllers. In time-critical situations where the speed supervision controller operates, the permanent magnet synchronous generator demonstrates very short speed response times, no overshoot, and no steady-state error (Fig. 12).

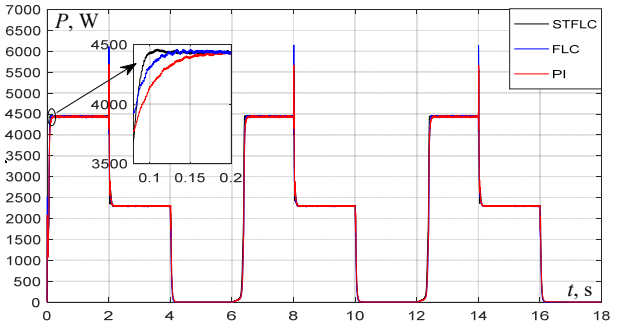

Fig. 12. Output power of the WT

Table 3 presents a comparison among 3 controllers. It's evident that the ST-FLC controller exhibits a shorter response time and reduced overshoot when compared to the other controllers. Additionally, the ST-FLC demonstrates smaller rise time and settling time in comparison to the other 2 controllers.

Table 3

MPPT WT performance metrics for PI, FLC and ST-FLC

Operation	Measure	PI	FLC	ST-FLC
MPPT WT	Setting time, s	0.193	0.124	0.104
	Rise time, s	0.123	0.102	0.077
	Overshoot, %	0.909	0.405	0.315

The ST-FLC has better tracking characteristics than other power control modules, the PV response time is very short compared to other controllers (Fig. 13).

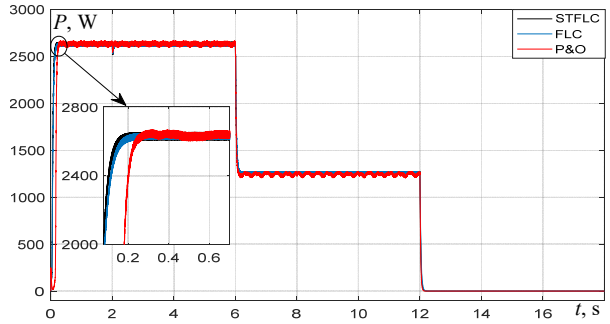

Fig. 13. Output power of the PV

Table 4 displays the outcomes of comparing the three controllers. The ST-FLC controller showcases shorter rise time and settling time. Moreover, both the ST-FLC and FLC controllers exhibit lesser overshoot when compared to the P&O controller.

Table 4

MPPT PV performance metrics for P&O, FLC and ST-FLC

Operation	Measure	P&O	FLC	ST-FLC
MPPT PV	Setting time, s	0.273	0.221	0.177
	Rise time, s	0.204	0.115	0.105
	Overshoot, %	0.506	0.189	0.189

A more detailed analysis of the steady-state power was carried out. A fast Fourier transform analysis has been used to calculate the Total Harmonic Distortion (THD) produced by the power. 20 cycles of the power were selected, starting at 0.2 s, the frequency fundamental and limited 50 Hz and 1000 Hz respectively to obtain a clear view of the THD spectrum. Tables 5, 6 show the power and THD spectrum for the 3 controllers.

Table 5

Phase a power THD of WT comparison

Controller	P, W	THD, %
PI	4395	3.94
FLC	4417	3.26
ST-FLC	4425	2.29

Table 6

Phase a power THD of PV comparison

Controller	P, W	THD, %
P&O	2559	7.21
FLC	2582	6.21
ST-FLC	2591	5.46

The performance evaluation of the proposed strategy, encompassing control and optimization, utilized the selected profiles: wind velocity (Fig. 10), solar irradiance (Fig. 11), and load power (Fig. 14). Figures 15, 16 depict the voltage shape and SOC, respectively, showcasing fluctuations of increase and decrease. When the load power surpasses the power supplied by sources (PV, WT), both the voltage and battery SOC decrease (indicating battery discharge). Conversely, they increase when the load power is lower, allowing the sources to charge the battery. Figure 17 shows the maintenance of V_{dc} at the reference value. Moreover, the powers generated by PV, WT, and batteries are presented in Fig 18. The obtained results affirm the effectiveness of the proposed FLC-based strategy, clearly demonstrating the successful achievement of its objectives.

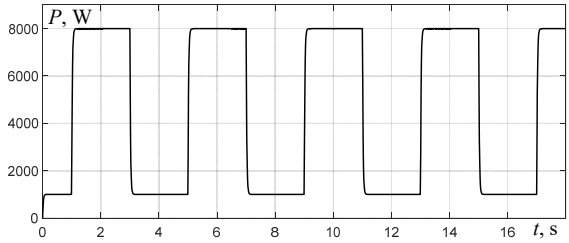

Fig. 14. Profile of the load power

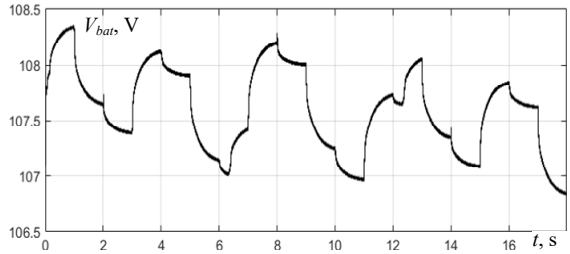

Fig. 15. Voltage of the battery

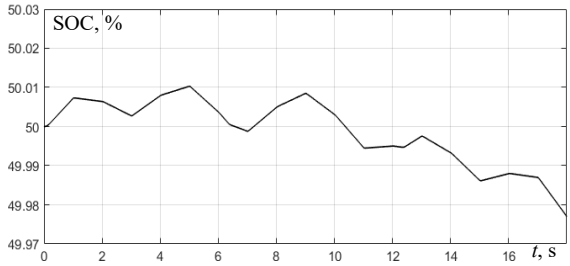

Fig. 16. The battery SOC

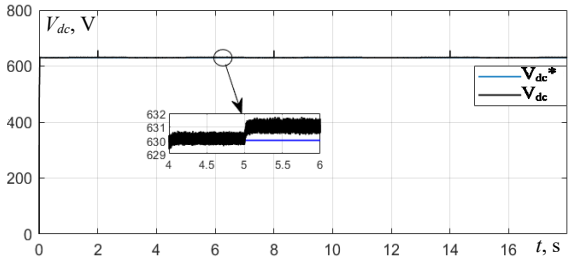

Fig. 17. Voltage V_{dc}

Conclusions.

1. This study explores the modelling, optimization, and control of a grid-connected HRES comprising two renewable sources (PV and WT) along with a storage system. The research conducts a comprehensive evaluation, highlighting a comparison between conventional and fuzzy-based approaches in controlling the MPPT. The FLC demonstrates notably enhanced performance compared to conventional methods, particularly beneficial when the model lacks clear definition, leveraging human experiential knowledge. The primary objective of this investigation revolves around assessing two advanced MPPT control strategies for WTs and PV systems: FLC, which utilizes error and its change to adjust control through fixed gain scaling factors, and ST-FLC, where the output gain dynamically adapts according to the prevailing system conditions.

2. The simulation outcomes demonstrate the superior performance of FLC over a conventional controller in terms of response speed and its capability to effectively track the maximum WT power. The ST-FLC strategy, employing a straightforward block design, exhibits robust performance and showcases commendable results compared to other utilized approaches.

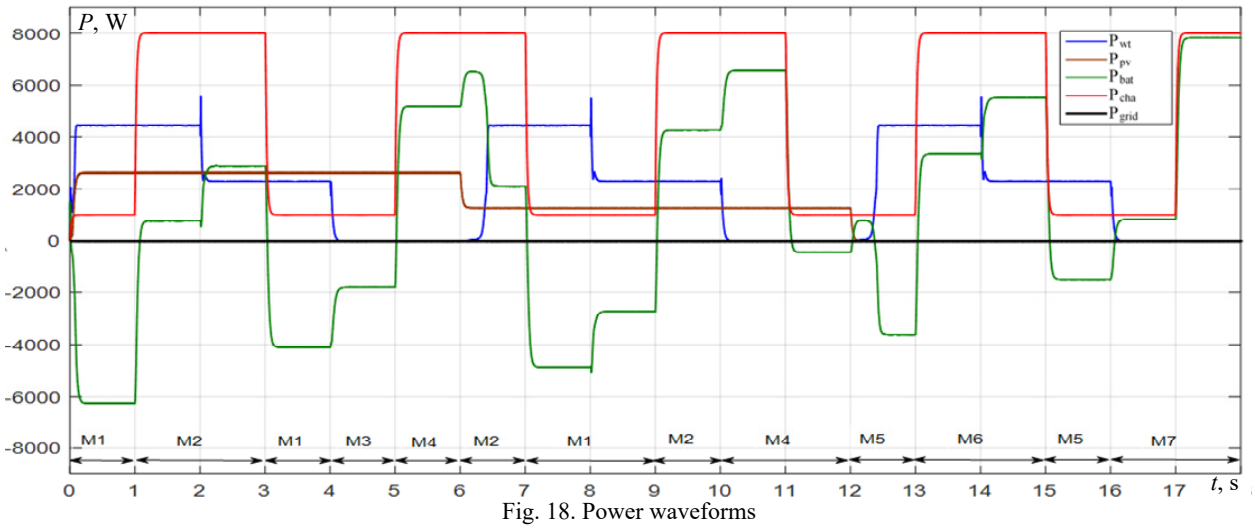

Fig. 18. Power waveforms

3. The introduced intelligent control strategy allows for diverse operating modes tailored to varying weather conditions, enabling seamless and rapid power supply from each source while considering the battery bank's state of charge. FLC serves a pivotal role in providing optimization and control within this framework.

4. These simulation findings unequivocally affirm the effectiveness and practicality of the proposed control strategy. The primary objectives, including substantial power gains, reduced battery load, and intelligent control, are successfully attained.

Conflict of interest. The authors declare that they have no conflicts of interest.

REFERENCES

1. *Renewables 2024. Global Status Report. Global Overview 2024*. Available at: https://www.ren21.net/gsr2024_GO_report (Accessed: 02 July 2024).

2. Muthukaruppasamy S., Dharmaprakash R., Sendilkumar S., Parimalasundar E. Enhancing off-grid wind energy systems with controlled inverter integration for improved power quality. *Electrical Engineering & Electromechanics*, 2024, no. 5, pp. 41-47. doi: https://doi.org/10.20998/2074-272X.2024.5.06.

3. Shivam K., Tzou J.-C., Wu S.-C. A multi-objective predictive energy management strategy for residential grid-connected PV-battery hybrid systems based on machine learning technique. *Energy Conversion and Management*, 2021, vol. 237, art. no. 114103. doi: https://doi.org/10.1016/j.enconman.2021.114103.

4. Lamzouri F.E.Z., Boufounas E.-M., Amrani A.El. Efficient energy management and robust power control of a stand-alone wind-photovoltaic hybrid system with battery storage. *Journal of Energy Storage*, 2021, vol. 42, art. no. 103044. doi: https://doi.org/10.1016/j.est.2021.103044.

5. Benlahbib B., Bouarroudj N., Mekhilef S., Abdeldjalil D., Abdelkrim T., Bouchafaa F., Lakhdari A. Experimental investigation of power management and control of a PV/wind/fuel cell/battery hybrid energy system microgrid. *International Journal of Hydrogen Energy*, 2020, vol. 45, no. 53, pp. 29110-29122. doi: https://doi.org/10.1016/j.ijhydene.2020.07.251.

6. Laxman B., Annamraju A., Srikanth N.V. A grey wolf optimized fuzzy logic based MPPT for shaded solar photovoltaic systems in microgrids. *International Journal of Hydrogen Energy*, 2021, vol. 46, no. 18, pp. 10653-10665. doi: https://doi.org/10.1016/j.ijhydene.2020.12.158.

7. Suresh G., Prasad D., Gopila M. An efficient approach based power flow management in smart grid system with hybrid renewable energy sources. *Renewable Energy Focus*, 2021, vol. 39, pp. 110-122. doi: https://doi.org/10.1016/j.ref.2021.07.009.

8. Bounechba H., Boussaid A., Bouzid A. Experimental validation of fuzzy logic controller based on voltage perturbation algorithm in battery storage photovoltaic system. *Electrical Engineering & Electromechanics*, 2024, no. 5, pp. 20-27. doi: https://doi.org/10.20998/2074-272X.2024.5.03.

9. Zerzouri N., Ben Si Ali N., Benalia N. A maximum power point tracking of a photovoltaic system connected to a three-phase grid using a variable step size perturb and observe algorithm. *Electrical Engineering & Electromechanics*, 2023, no. 5, pp. 37-46. doi: https://doi.org/10.20998/2074-272X.2023.5.06.

10. Jately V., Azzopardi B., Joshi J., Venkateswaran V.B., Sharma A., Arora S. Experimental Analysis of hill-climbing MPPT algorithms under low irradiance levels. *Renewable and Sustainable Energy Reviews*, 2021, vol. 150, art. no. 111467. doi: https://doi.org/10.1016/j.rser.2021.111467.

11. Louarem S., Kebbab F.Z., Salhi H., Nouri H. A comparative study of maximum power point tracking techniques for a photovoltaic grid-connected system. *Electrical Engineering & Electromechanics*, 2022, no. 4, pp. 27-33. doi: https://doi.org/10.20998/2074-272X.2022.4.04.

12. Kaddache M., Drid S., Khemis A., Rahem D., Chrifi-Alaoui L. Maximum power point tracking improvement using type-2 fuzzy controller for wind system based on the double fed induction generator. *Electrical Engineering & Electromechanics*, 2024, no. 2, pp. 61-66. doi: https://doi.org/10.20998/2074-272X.2024.2.09.

13. Mahgoun M.S., Badoud A.E. New design and comparative study via two techniques for wind energy conversion system. *Electrical Engineering & Electromechanics*, 2021, no. 3, pp. 18-24. doi: https://doi.org/10.20998/2074-272X.2021.3.03.

14. Farah N., Talib M.H.N., Mohd Shah N.S., Abdullah Q., Ibrahim Z., Lazi J.B.M., Jidin A. A Novel Self-Tuning Fuzzy Logic Controller Based Induction Motor Drive System: An Experimental Approach. *IEEE Access*, 2019, no. 7, pp. 68172-68184. doi: https://doi.org/10.1109/ACCESS.2019.2916087.

15. Marugán A.P., Márquez F.P.G., Perez J.M.P., Ruiz-Hernández D. A survey of artificial neural network in wind energy systems. *Applied Energy*, 2018, vol. 228, pp. 1822-1836. doi: https://doi.org/10.1016/j.apenergy.2018.07.084.

16. Mansouri M., Bey M., Hassaine S., Larbi M., Allaoui T., Denai M. Genetic algorithm optimized robust nonlinear observer for a wind turbine system based on permanent magnet synchronous generator. *ISA Transactions*, 2022, vol. 129, pp. 230-242. doi: https://doi.org/10.1016/j.isatra.2022.02.004.

17. Guentri H., Allaoui T., Mekki M., Denai M. Power management and control of a photovoltaic system with hybrid

battery-supercapacitor energy storage based on heuristics methods. *Journal of Energy Storage*, 2021, vol. 39, art. no. 102578. doi: https://doi.org/10.1016/j.est.2021.102578.
18. Sabhi K., Talea M., Bahri H., Dani S. Integrating dual active bridge DC-DC converters: a novel energy management approach for hybrid renewable energy systems. *Electrical Engineering & Electromechanics*, 2025, no. 2, pp. 39-47. doi: https://doi.org/10.20998/2074-272X.2025.2.06.
19. Ayat Y., Badoud A.E., Mekhilef S., Gassab S. Energy management based on a fuzzy controller of a photovoltaic/fuel cell/Li-ion battery/supercapacitor for unpredictable, fluctuating, high-dynamic three-phase AC load. *Electrical Engineering & Electromechanics*, 2023, no. 3, pp. 66-75. doi: https://doi.org/10.20998/2074-272X.2023.3.10.
20. Sharma R.K., Mudaliyar S., Mishra S. A DC Droop-Based Optimal Dispatch Control and Power Management of Hybrid Photovoltaic-Battery and Diesel Generator Standalone AC/DC System. *IEEE Systems Journal*, 2021, vol. 15, no. 2, pp. 3012-3023. doi: https://doi.org/10.1109/JSYST.2020.3032887.
21. Kamel A.A., Rezk H., Abdelkareem M.A. Enhancing the operation of fuel cell-photovoltaic-battery-supercapacitor renewable system through a hybrid energy management strategy. *International Journal of Hydrogen Energy*, 2021, vol. 46, no. 8, pp. 6061-6075. doi: https://doi.org/10.1016/j.ijhydene.2020.06.052.
22. Ali Moussa M., Derrouazin A., Latroch M., Aillerie M. A hybrid renewable energy production system using a smart controller based on fuzzy logic. *Electrical Engineering & Electromechanics*, 2022, no. 3, pp. 46-50. doi: https://doi.org/10.20998/2074-272X.2022.3.07.
23. Toghani Holari Y., Taher S.A., Mehrasa M. Power management using robust control strategy in hybrid microgrid for both grid-connected and islanding modes. *Journal of Energy Storage*, 2021, vol. 39, art. no. 102600. doi: https://doi.org/10.1016/j.est.2021.102600.
24. Charrouf O., Betka A., Abdeddaim S., Ghamri A. Artificial Neural Network power manager for hybrid PV-wind desalination system. *Mathematics and Computers in Simulation*, 2020, vol. 167, pp. 443-460. doi: https://doi.org/10.1016/j.matcom.2019.09.005.
25. Taghdisi M., Balochian S. Maximum Power Point Tracking of Variable-Speed Wind Turbines Using Self-Tuning Fuzzy PID. *Technology and Economics of Smart Grids and Sustainable Energy*, 2020, vol. 5, no. 1, art. no. 13. doi: https://doi.org/10.1007/s40866-020-00087-3.
26. Roumila Z., Rekioua D., Rekioua T. Energy management based fuzzy logic controller of hybrid system wind/photovoltaic/diesel with storage battery. *International Journal of Hydrogen Energy*, 2017, vol. 42, no. 30, pp. 19525-19535. doi: https://doi.org/10.1016/j.ijhydene.2017.06.006.
27. Singh P., Lather J.S. Power management and control of a grid-independent DC microgrid with hybrid energy storage system. *Sustainable Energy Technologies and Assessments*, 2021, vol. 43, art. no. 100924. doi: https://doi.org/10.1016/j.seta.2020.100924.

Received 10.11.2024
Accepted 08.01.2025
Published 02.05.2025

H. Chaib[1]*, PhD Student,*
S. Hassaine[1]*, PhD, Professor,*
Y. Mihoub[1]*, PhD, Associate Professor,*
S. Moreau[2]*, PhD, Associate Professor,*
[1] Laboratory of Energy Engineering and Computer Engineering, University of Tiaret, Algeria,
e-mail: housseyn.chaib@univ-tiaret.dz (Corresponding Author); said.hassaine@univ-tiaret.dz; youcef.mihoub@univ-tiaret.dz
[2] Laboratory of Informatics and Automatic Systems (LIAS), Poitiers University, France,
e-mail: sandrine.moreau@univ-poitiers.fr

How to cite this article:
Chaib H., Hassaine S., Mihoub Y., Moreau S. Intelligent power control strategy based on self-tuning fuzzy MPPT for grid-connected hybrid system. *Electrical Engineering & Electromechanics*, 2025, no. 3, pp. 23-30. doi: https://doi.org/10.20998/2074-272X.2025.3.04